







Article

Electrochemical Sensitivity Improvement by the Cooperation between Pt and Ru for Total Antioxidant Evaluation in Natural Extracts

Gustavo Carvalho Diniz ¹, Vinicius Tribuzi Rodrigues Pinheiro Gomes ² , Marcelo de Assis ³ , Santiago José Alejandro Figueroa ⁴ , Igor Ferreira Torquato ⁴ , Luiz Gustavo de Freitas Borges ⁴, Hector Aguilar Vitorino ^{5,*} , Roberto Batista de Lima ⁶, Marco Aurélio Suller Garcia ⁶  and Isaide de Araujo Rodrigues ^{1,6}

- ¹ Programa de Pós-Graduação em Química (PPGQ), Instituto Federal de Educação, Ciências e Tecnologia do Maranhão (IFMA), São Luís 65030-005, MA, Brazil; isaide.rodrigues@ufma.br (I.d.A.R.)
 - ² Departamento de Física, Laboratório de Óptica, Laser e Fotônica, Universidade Federal de São Carlos, São Carlos 13565-905, SP, Brazil
 - ³ Department of Analytical and Physical Chemistry, University Jaume I (UJI), 12071 Castelló, Spain
 - ⁴ Brazilian Synchrotron Light Laboratory (LNLS), Brazilian Center for Research in Energy and Materials (CNPEM), Campinas 13083-970, SP, Brazil
 - ⁵ Centro de Investigación en Biodiversidad para la Salud, Universidad Privada Norbert Wiener, Lima 15046, Peru
 - ⁶ Departamento de Química, CCET, Universidade Federal do Maranhão, São Luís 65080-805, MA, Brazil; rb.lima@ufma.br (R.B.d.L.); marco.suller@ufma.br (M.A.S.G.)
- * Correspondence: havitorino@gmail.com



Citation: Diniz, G.C.; Pinheiro Gomes, V.T.R.; de Assis, M.; Alejandro Figueroa, S.J.; Ferreira Torquato, I.; de Freitas Borges, L.G.; Aguilar Vitorino, H.; de Lima, R.B.; Suller Garcia, M.A.; de Araujo Rodrigues, I. Electrochemical Sensitivity Improvement by the Cooperation between Pt and Ru for Total Antioxidant Evaluation in Natural Extracts. *Chemosensors* **2023**, *11*, 314. <https://doi.org/10.3390/chemosensors11060314>

Academic Editor: Jian Ling

Received: 16 March 2023

Revised: 4 April 2023

Accepted: 14 April 2023

Published: 23 May 2023



Copyright: © 2023 by the authors. Licensee MDPI, Basel, Switzerland. This article is an open access article distributed under the terms and conditions of the Creative Commons Attribution (CC BY) license (<https://creativecommons.org/licenses/by/4.0/>).

Abstract: Herein, a straightforward electrochemical method was used to evaluate the total phenolic antioxidant capacity in natural extracts prepared from pomegranate, hibiscus, and pitaya. In light of this, the well-known electrochemical index (EI), a screening protocol for natural antioxidant properties evaluation, was determined using differential pulse voltammetry. Initially considering rutin and catechin as standards, we found that the system's sensitivity greatly increased by using platinum (Pt) and platinum/ruthenium (Pt/Ru) nanoparticles (NPs) immobilized on Vulcan XC-72 to modify screen-printed carbon electrodes (SPCEs). When such modifications were applied to natural fruit/plant extracts, their electrochemical ability proved highly superior to the bare SPCE, even considering a very small amount of materials for electrode preparation. However, with an optimized ratio, the bimetallic counterpart was more sensitive to detection. When the pomegranate extract was used, for example, EI values of 52.51 ± 6.00 and $104.79 \pm 6.89 \mu\text{A/V}$ were obtained using Pt and Pt/Ru (with an optimized ratio) electrocatalysts, showing the remarkable sensitivity increase obtained in our bimetallic protocol. Thus, based on physicochemical and electrochemical characterizations, we found that the ruthenium content was essential for the achievements. In due course, XPS analysis suggested that the $\text{Pt}^{2+}/\text{Pt}^0$ species ratio could have improved the system's sensitivity, which significantly changed when ruthenium was used in the material.

Keywords: antioxidant evaluation; electrochemical index; SPCE; noble metals

1. Introduction

Plant-based food is often rich in bioactive compounds that impact humans' physiological and cellular activities. Therefore, the regular consumption of fruits, vegetables, and antioxidant-rich beverages can potentially reduce pathological risk factors and may help treat certain diseases [1]. In this scenario, it is essential to point out that the leading representative of such components is the group of phenolic compounds, with more than ten thousand structures cataloged. Due to their importance, they are very well studied,

and it is suggested that their antioxidant activity originates from their hydroxyl radicals [2]; however, many considerations may be derived from their structure and in vivo complex interactions, which make them exciting but challenging [3].

Antioxidants act as free radical scavengers (deactivators of reactive oxygen and nitrogen species), inhibitors of lipid peroxidation and 'DNA' oxidation, among other functions. Although free radicals are naturally generated by the human body and are involved in critical metabolic processes [4], the excessive production of these free radicals favors a homeostatic imbalance known as oxidative stress, which causes damage to essential biomolecules and is associated with inflammatory processes and chronic diseases [5]. Therefore, antioxidant compounds are of great importance to the food and pharmaceutical industries and can be applied in product quality control and conservation [6].

After highlighting their importance, it is vital that the antioxidant capacity of natural sources be evaluated as they may assist in designing novel foods with better health potential [7]. Thus, there are several ways to assess the antioxidant activity of a given substance, ranging from chemical tests using lipid substrates to more sophisticated assays using a wide range of instrumental techniques [8]. However, electrochemical methods are widely used to quantify antioxidant compounds due to their high selectivity and sensitivity; along with these characteristics, electrochemistry offers fast and low-cost analyses [9].

The electrodes can be modified with different materials holding specific properties that allow synergetic abilities [10]. Surface area gain using NPs also directly affects the electrochemically active area, an important issue to pursue in such systems. Thus, the choice of modifiers is essential to optimize physical and chemical properties for advanced sensing properties [11]. Noble metal NPs can be efficiently used on the surface of carbon-based electrodes, but their use must be reduced and optimized due to their cost. Platinum NPs stand out due to their high electrocatalytic activity; when combined with carbon-based materials, their area greatly increases, apart from electrocatalytic properties that may arise (such electrocatalyst—Pt/C—is highly used in several electrochemical methods) [12,13]. However, a suitable combination with other noble metals would enhance electrical conductivity and fast electron transfer; Ru NPs may play this role and will be studied herein [14,15].

Thus, the total phenolic antioxidant capacity in natural extracts prepared from pomegranate, hibiscus, and pitaya will be evaluated by EI using differential pulse voltammetry as a fast, suitable, and straightforward method. We also designed Pt and Pt/Ru-based electrocatalysts supported on Vulcan XC-72, which were used to modify SPCEs used in the sensing system. Based on physicochemical and electrochemical characterizations, we found that the Ru content was essential for the outcomes, improving systems that regularly use commercial Pt/C materials as a rule of thumb for electrochemical techniques. XPS analysis also brought insights related to the Pt^{2+}/Pt^0 species ratio change with the Ru addition, which could have improved the systems' sensitivity.

2. Experimental Section

The solutions and washing procedures were performed with deionized water (resistivity of 18.2 m Ω cm Millipore[®], Billerica, MA, USA). Before analysis, the glassware was soaked in an alkaline solution of 0.1% potassium permanganate (*v/v*) for 24 h, followed by washing with a piranha solution (comprised of H₂SO₄ and H₂O₂ in a proportion of 7:1), and maintained in an ultrasound bath for 20 min with deionized water. Finally, an abundant rinse with water was performed before drying.

The Vulcan XC-72 carbon powder was purchased from Cabot Corporation (Boston, MA, USA), and H₂PtCl₆·3H₂O, RuCl₃·3H₂O, H₂SO₄, glycol ethylene, methanol, and KCl were acquired from Merck (Darmstadt, Germany); SnCl₂·2H₂O, KI, HCl, and HNO₃ were purchased from Isofar (Rio de Janeiro, Brazil). Catechin and rutin were purchased from Sigma-Aldrich (MilliporeSigma, St. Louis, MO, USA), with purity greater than 98% and 94%, respectively.

2.1. Pretreatment of Vulcan XC-72 Carbon

The treatment of Vulcan XC-72 carbon was performed before the NPs' immobilization, aiming to increase the material's current capacity. Typically, 1.0 g of the powder was dispersed in 250 mL of 5.0 M HNO₃ using a 500 mL round bottom flask. Then, the mixture was kept under ultrasound for 1 h before reflux for 5 h at 80 °C. The obtained material was filtered off and washed with deionized water until the pH was neutral [16].

2.2. Pt and Pt/Ru-Based Electrocatalysts Synthesis

The materials were prepared according to the literature with modifications [17]. In a typical synthesis, the metal precursor—H₂PtCl₆·3H₂O—(or precursors, when bimetallic counterparts were prepared; in the present procedure, RuCl₃·3H₂O) was added to 50 mL of ethylene glycol/water volume ratio (3:1) containing Vulcan XC-72 carbon and refluxed for 2 h at 80 °C before filtering and washing with deionized water three times. The resulting materials were left to dry under ambient conditions for 12 h before utilization. The metal loading was calculated to make up 20 wt.%. The bimetallic catalysts were prepared considering the following Pt/Ru metal ratios: 80:20 and 60:40 [18].

2.3. Sample Preparation

The extracts were prepared using pitaya, hibiscus, and pomegranate purchased in a local market in São Luís, Maranhão. They were frozen for preservation up to the preparation of the extract to be used in electrochemical analyses. Typically, 10 g of each sample was macerated for 10 min before filtration (200 mesh filter) to obtain a liquid extract. Then, the extracted liquid of each sample was mixed with an extraction solution (comprised of HCl-acidified methanol that was prepared using 1% (v/v) of concentrated HCl) in the proportion of 1 mL of each sample to 4 mL of extraction solution. Then, 2 mL of the final solution was mixed with 10 mL of the electrolyte, and the analyses were performed [9,19].

2.4. Electrochemical Measurements

The electrochemical studies carried out herein were performed using Autolab PG-STAT 302 N potentiostat equipped with a FRA2 impedance module (Metrohm, Herisau, Switzerland). The data was acquired using screen-printed carbon electrodes (SPCEs, DropSens, DRP-110). To perform our experiment, we needed to modify the SPCEs, as follows: 2.5 mg of the electrocatalyst was added to 0.5 mL of methanol with 0.05 mL Nafion[®] 5.0 wt.% and 0.7 mL of deionized water. An ultrasound device was used for 20 min to disperse the mixture. After this procedure, 10 µL of the dispersion was drop-casted onto the work electrode surface. Every analysis was carried out at pH 2.2 buffer HCl/KCl, 0.2 mol L⁻¹.

Differential pulse voltammetry (DPV) and Cyclic voltammetry (CV) evaluations were performed in 0.2 mol L⁻¹ HCl/KCl electrolyte. A regular electrochemical Impedance Spectroscopy (EIS) procedure was accomplished in 0.1 mol L⁻¹ KCl with 5 mmol L⁻¹ Fe(CN)₆^{3-/4-} at room temperature [20]. The electrochemical index (EI) was used to study parameters of peak potential (E_p —donor capacity of the species at 0 V) and peak current (I_p —number of electroactive species) [9,21]. The EI is calculated as follows:

$$EI = \frac{I_{p1}}{E_{p1}} + \frac{I_{p2}}{E_{p2}} + \dots + \frac{I_{pn}}{E_{pn}}$$

The electrochemical surface area (ECSA) of the electrodes was obtained based on the following equation:

$$ECSA = \frac{A_H}{vQ_HM_{Pt}}$$

A_H is the Hydrogen adsorption area, v is the scan speed, Q_H is the charge density for polycrystalline Pt with a value of 210 and platinum mass, M_{Pt} is platinum mass. The unit of measurement used was Cm²g_{Pt}⁻¹ [16,17].

2.5. Physico-Chemical Characterizations

The materials' crystalline structures were studied using X-ray diffraction (XRD). The spectra were obtained using an ULTIMA IV diffractogram (Rigaku, Shibuya, Tokyo) with Cu K α radiation (1.54060 Å) [22]. The equipment was set to work for 10–90° 2 θ , at 3°/min speed. The crystallite sizes were calculated from the Scherrer equation:

$$\tau = \frac{K \lambda}{\beta \cos \theta}$$

where τ is the mean size of the crystalline domains, K is a dimensionless shape factor, λ is the X-ray wavelength, β is the line broadening at half the maximum intensity (FWHM), and θ is the Bragg angle.

Transmission electron microscopy (TEM) images were obtained using JEOL JEM 2100 microscope (operating at 110 kV). The NPs sizes were determined using the open-source image processing program ImageJ [23]. Samples for microscopy were prepared by drop-casting an isopropanol suspension of the materials over a grid comprised of carbon-coated copper, followed by drying under ambient conditions. X-ray photoemission spectroscopy (XPS) spectra were obtained with a Thermo Scientific K-alpha spectrometer, with a monochromatic Al K-alpha radiation source ($E = 1486.68$ eV) operating at 12 kV; the X-ray spot size was 400 μm , and the analyzer pass energy was set on 50 eV. Charge compensation was achieved using the FG03 flood gun using a combination of low-energy electrons and the ion flood source. The data was analyzed by CasaXPS software version 2.3.15 (Casa Software Ltd., Teignmouth, UK) [24].

3. Results and Discussion

3.1. Physico-Chemical and Electrochemical Characterizations

We started our investigations by analyzing the synthesis of the electrocatalysts. The Vulcan XC-72 powder was treated with 5 mol·L⁻¹ HNO₃ to improve its capacity current before NPs immobilization, which proved to be a good strategy. Such a process can also eliminate impurities and enhance the surface area, which are interesting features to seek in NPs immobilization procedures. Once we aimed to obtain small NPs, we selected the well-established polyol method to guarantee their size homogeneity. To this end, H₂PtCl₆·3H₂O (and RuCl₃·3H₂O for the bimetallic electrocatalysts) was used as a metal precursor and ethylene glycol as both a solvent and reducing agent.

One can notice that all the TEM images show the disordered structure of amorphous carbon, in which the NPs are immobilized (Figure 1). Figure 1A reveals that the Pt/C presents a high dispersion of the NPs all over the support, with some agglomeration points; higher magnification shows the formation of individual NPs (Figure 1B). Figure S1A,B shows well-ordered crystallite planes with d-spacings of 2.28 Å due to {111} lattice fringes in face-centered cubic Pt; the NPs presented 4.3 ± 3.6 nm in diameter, although a small number of the NPs was much higher (Figure 1C). At first glance, the bimetallic electrocatalyst comprised of Pt:Ru 80:20 (Pt₈₀Ru₂₀/C) seems to present the formation of larger-sized NPs, as displayed in Figure 1D; however, the NPs' disposition was concentrated in some support sites, as observed at higher magnification (Figure 1E). The material presented d-spacings of 1.84 and 2.28 Å, regarding cubic Pt with {200} and {111} lattice fringes, respectively; also, 2.34 Å, due to the Ru hexagonal {100} (Figure S1C,D). Thus, we cannot suggest an alloy formation; on the contrary, the Ru e Pt atoms were very close to each other in an aleatory manner. The NPs' sizes were performed considering the structure as a whole, showing dimensions of 4.1 ± 2.4 nm (Figure 1F).

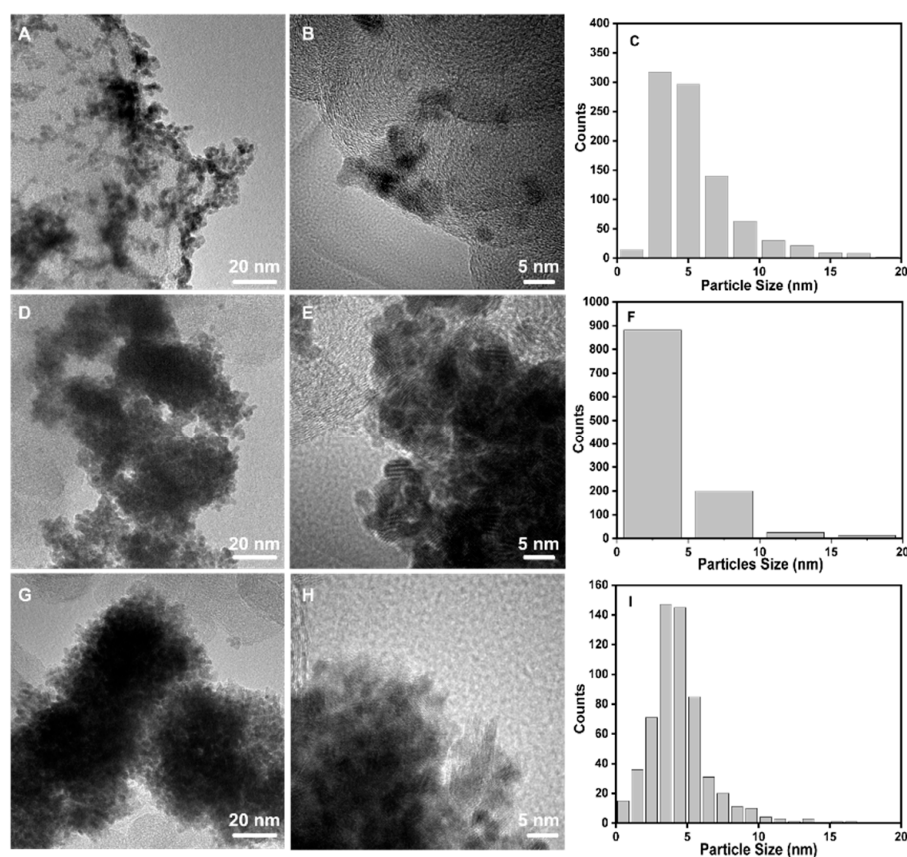


Figure 1. TEM of (A,B) Pt/C, (D,E) Pt₈₀Ru₂₀/C, and (G,H) Pt₆₀Ru₄₀/C electrocatalysts. Histograms of the (C) Pt/C, (F) Pt₈₀Ru₂₀/C, and (I) Pt₆₀Ru₄₀/C electrocatalysts.

The same evidence was achieved for the Pt:Ru 60:40 (Pt₆₀Ru₄₀/C) electrocatalyst, with particles' size of 4.1 ± 2.6 nm and d-spacings of cubic Pt of 2.01 Å {200} and 2.26 Å {111}, and hexagonal Ru of 2.05 Å {101} and 4.23 Å {002} (Figure 1G–I and Figure S1D,E). Such findings were expected regarding the chosen synthesis procedure. Nevertheless, the synergy among the different metals may be other among the samples. High-index facets tend to present higher catalytic activity than low-index ones due to higher surface energy. EDS analysis showed that the impregnation over carbon was effective, i.e., followed by the nominal preparation (Table 1). The 20.0 wt.% Pt loading was also achieved for the monometallic electrocatalyst.

Table 1. Comparison between the nominal and EDS metal ratios.

| Electrocatalysts | Nominal Ratio (%) | | Atomic Ratio (%) | |
|--|-------------------|----|------------------|----|
| Pt ₈₀ %Ru ₂₀ %/C | 80 | 20 | 81 | 19 |
| Pt ₆₀ %Ru ₄₀ %/C | 60 | 40 | 60 | 40 |

The X-ray diffraction patterns of catalysts are shown in Figure 2. Due to the nature of the supporting material, the (002) peak of the graphite basal plane is present in all samples [20]. One can also notice that the Pt/C and Pt₈₀Ru₂₀/C samples presented similar characteristics: distinct peaks could be indexed to (111), (200), (220), and (311) planes ($2\theta = 40^\circ, 47^\circ, 68^\circ$ and 82°) for face-centered cubic Pt, which corroborates the microscopy analyses presented before for these materials. Peaks regarding Ru were not observed, probably due to its very low concentration. However, it is noteworthy that apparent changes in the XRD pattern are visible with increasing Ru concentration.

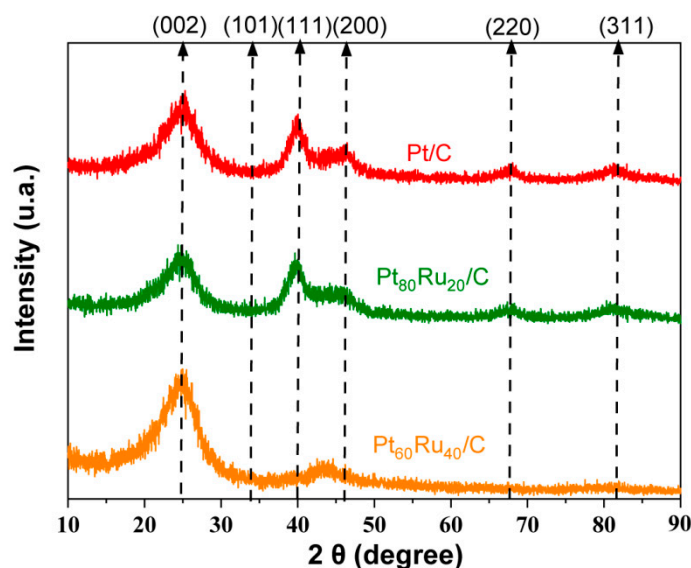


Figure 2. XRD patterns of the Pt/C, Pt₈₀Ru₂₀/C, and Pt₆₀Ru₄₀/C electrocatalysts.

With the augmentation of this metal to compose 40.0 wt.%, an evident change in crystallinity was detected, with broader peaks. The Pt {111} and {200} planes were also not available, different from those observed in the microscopy analyses; instead, a peak at $2\theta = 43.6^\circ$ related to Ru (101) is consistent and also observed in the microscopy analyses. Herein, the importance of the XRD results is noticeable: Pt₆₀Ru₄₀/C presents some substantial peak pattern changes, probably related to the increased amount of Ru instead of alloy formation. Thus, although some degree of alloying is possible, the NPs formation was more likely to be spatially close to a mixture of metallic phases, corroborating our previous conclusions. Notably, the NPs sizes obtained in the TEM images are similar to those observed by crystalline measurements calculated by the Scherrer equation (Table S1).

The electrochemically active area (ECSA) was calculated for the modified electrodes, and these results are presented in Table 2. One can notice that the Ru₄₀Pt₆₀/C modified electrode gave the higher EASA, followed by the Ru₂₀Pt₈₀/C modified electrode.

Table 2. Electrochemically active surface area for the modified electrodes.

| Electrodes | Active Electrochemical Area ($\text{Cm}^2 \text{g}_{\text{Pt}}^{-1}$) |
|--------------------------------------|---|
| Pt/C | 22.60 |
| Pt ₈₀ Ru ₂₀ /C | 21.43 |
| Pt ₆₀ Ru ₄₀ /C | 41.42 |

The results of the CVs are presented in Figure 3A, considering the ECSA calculated before. In the Pt/C modified-electrode, the potentials from -0.5 V to -0.2 V are attributed to the Pt-hydrogen adsorption/desorption region [20], while the potentials centered at 0.15 V and 0.87 V are related to PtO_x formation and reduction, respectively. The region comprising the electrical double layer ranges from -0.1 V to $+0.5$ V. When alloying the catalyst with 20.0 at.% Ru, we can see a shift of the reduction peak to lower potential, which could be due to PtO_x and RuO_x species; however, 40.0 at.% Ru caused a reduction peak shift to a higher potential. In addition, a notorious current decrease in the Ru content was observed.

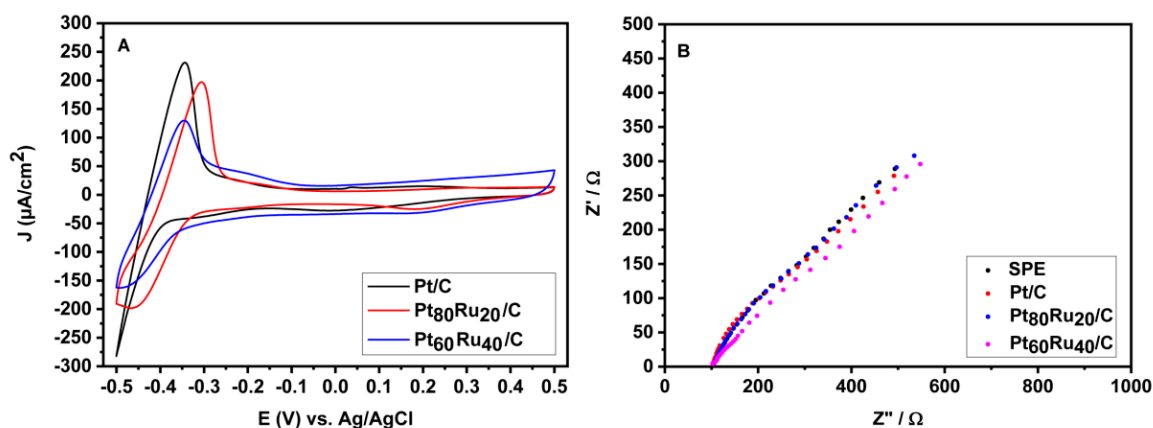


Figure 3. (A) CV of Pt/C, Ru₂₀Pt₈₀/C, and Ru₄₀Pt₆₀/C in 0.2 mol L⁻¹ HCl/KCl solution, recorded in a potential range of -0.5 V to 0.5 V. (B) Electrochemical impedance spectroscopy performed on SPCE, Pt/C, Ru₂₀%Pt₈₀%/C, and Ru₄₀%Pt₆₀%/C electrodes.

EIS was performed to assess the electrochemical performance of the modified electrodes. For this, the plotting of the real (Z') and imaginary ($-Z''$) components was performed, resulting in two distinct regions in a Nyquist plot, according to Figure 3B. The resistances observed were: 145.5 Ω , 125.5 Ω , 103.5 Ω , and 95 Ω for the SPCE, Pt/C, Pt₆₀Ru₄₀/C, Pt₈₀Ru₂₀/C modified-electrodes, respectively. Interestingly, the catalysts with Ru presented lower resistances, suggesting that the final catalysts' structure is directly related to the mixing process and quantity, finding an optimum improved electrical conductivity. Such results follow the data obtained by previous characterizations.

3.2. Antioxidant Evaluation by DPV and EI

Low selectivity and sensitivity are expected on unmodified carbon electrodes. There are several explanations for these results, such as low kinetics of the electrochemical reactions, high background current, and a need for overpotentials [25]. Based on the previous electrochemical characteristics herein presented, we are prone to believe that such drawbacks can be partially overcome by using the prepared catalysts, and they can provide considerable differences when applied to phenolic content assessment. For such analyses, rutin and catechin were chosen as standards.

When unmodified SPCE was used for the electrochemical studies (Figure 4A), one can notice that two peaks are observed for the catechin sample (10 μ M) centered at 0.36 and 0.62 V. At the same time, the rutin (10 μ M) presents one peak centered at 0.40 V. Performing the same experiments with the modified SPCE electrode with our electrocatalysts, remarkable differences were noticed. Using catechin (Figure 4B), the Pt/C-modified electrode showed a peak at 0.49 V, displaying some potential shift; however, without the modification, two signals were noticed. When the bimetallic counterparts were used, three signals were detected. Peaks at 0.06, 0.35, and 0.62 V were obtained for the Ru₂₀Pt₈₀/C material, and signals at 0.14, 0.34, and 0.58 V for the Ru₄₀Pt₆₀/C electrocatalyst. These results show that the SPCE modification was essential for the sensing behavior for detecting the compound, indicating that the bimetallic catalysts were more sensitive to detection. Nevertheless, the current density with less quantity of Ru was higher. Similar conclusions could be obtained when the same was performed using rutin as a standard (Figure 4C). For the Pt/C-modified SPCE, only one signal was detected (0.44 V), with a shift in the potential compared to the bare SPCE (0.40 V). The Ru₂₀Pt₈₀/C material showed two resolved peaks at 0.18 and 0.43 V, while the Ru₄₀Pt₆₀/C electrocatalyst showed two clear signals at 0.42 and 0.63 V and one broad signal between 0.00 and 0.25 V.

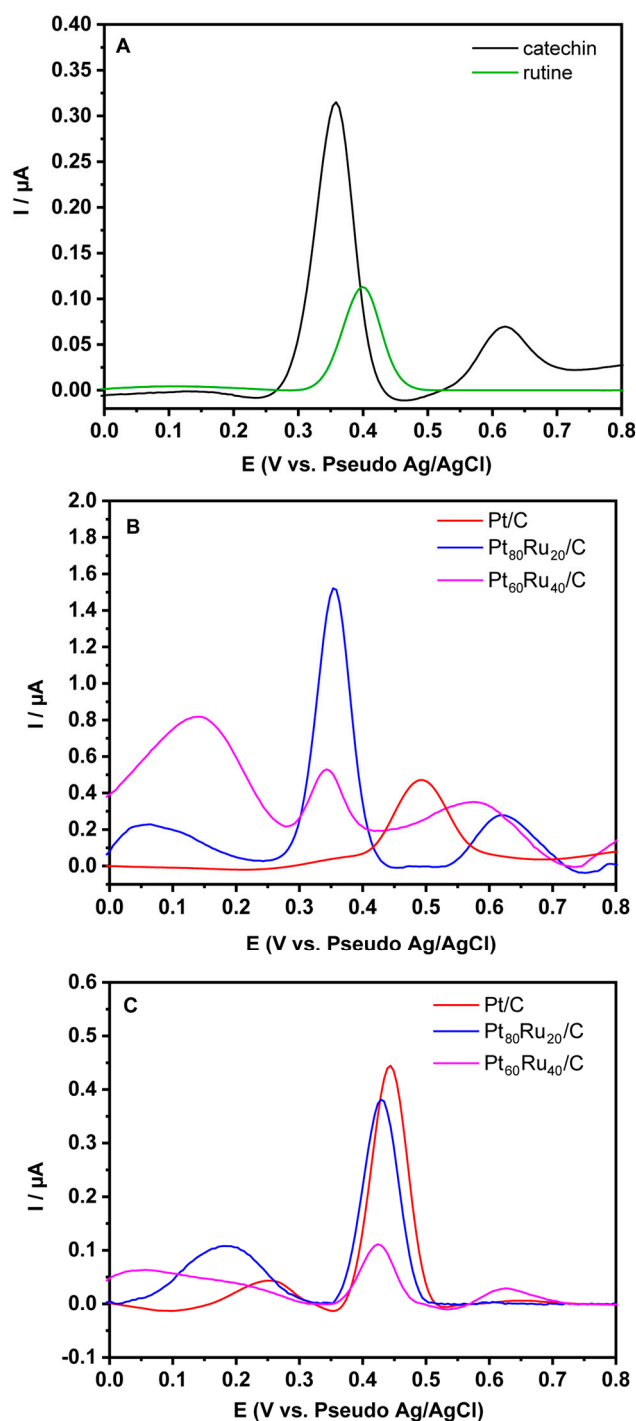


Figure 4. DPV tests performed with the (A) bare SPCE, (B) catechin, and (C) rutin standards in HCl/KCl 0.2 mol L^{-1} , $v = 10 \text{ mV/s}$.

The electrochemical index (EI) is another critical parameter in the antioxidant field despite the potential differences observed. Such information is regarded as the total antioxidant capacity of a molecule, i.e., its ability to donate electrons and protons [9]. The EI obtained for the standards showed remarkable differences: using the unmodified SPCE, catechin, and rutin presented 0.99 and $0.27 \mu\text{A/V}$, respectively. Pt/C-modified SPCE gave 21.74 and $19.93 \mu\text{A/V}$ for catechin and rutin, respectively. The bimetallic counterparts showed improvements: $488.64 \mu\text{A/V}$ ($\text{Pt}_{80}\text{Ru}_{20}/\text{C}$) and $31.18 \mu\text{A/V}$ ($\text{Pt}_{60}\text{Ru}_{40}/\text{C}$) for catechin and $157.93 \mu\text{A/V}$ ($\text{Pt}_{80}\text{Ru}_{20}/\text{C}$) and $57.10 \mu\text{A/V}$ ($\text{Pt}_{60}\text{Ru}_{40}/\text{C}$) for rutin. Such

results indicated that the samples were more sensitive to antioxidant detection in the bimetallic materials.

Based on the data obtained, we performed experiments with natural samples prepared by extracts of fruits/flowers (hibiscus, pitaya, and pomegranate). For the unmodified electrodes, the following potentials were observed: 0.14, 0.36, and 0.50 V (pomegranate), 0.20, 0.39, and 0.62 V (hibiscus), and 0.22, 0.34, and 0.53 V (pitaya). One can notice that these values are within the ranges obtained previously for the rutin and catechin standards; therefore, they can be associated with the presence of these phenolic compounds. The SPCE presented the following EI: $20.55 \pm 3.59 \mu\text{A/V}$ (pomegranate), $10.36 \pm 1.22 \mu\text{A/V}$ (hibiscus), and $11.28 \pm 0.39 \mu\text{A/V}$ (pitaya). It is important to highlight that this methodology is used in the literature for similar studies [26].

The modified electrodes were tested at the same conditions; the results are shown in Table 3 and Figure 5. All the modified electrodes showed similar potential; however, EI values were quite different. For pitaya (Figure 5A) and hibiscus (Figure 5B) extracts, the following order of EI was obtained: $\text{Pt}_{60\%}\text{Ru}_{40\%}/\text{C} > \text{Pt}_{80\%}\text{Ru}_{20\%}/\text{C} > \text{Pt}/\text{C}$. Nevertheless, the order for pomegranate was $\text{Pt}_{80\%}\text{Ru}_{20\%}/\text{C} > \text{Pt}_{60\%}\text{Ru}_{40\%}/\text{C} > \text{Pt}/\text{C}$ (Figure 5C). It is noticeable that the modified electrode with bimetallic materials was essential to evaluate the antioxidant content most accurately. Although the analyses with pomegranate showed that the $\text{Pt}_{80\%}\text{Ru}_{20\%}/\text{C}$ had improved performance, the other two extract analyses also delivered the information that the $\text{Pt}_{60\%}\text{Ru}_{40\%}/\text{C}$ could be considered as the optimized material for the analysis. To evaluate the performance of the materials comprehensively, we decided to analyze the XPS data comparing the $\text{Pt}_{60\%}\text{Ru}_{40\%}/\text{C}$ and Pt/C electrodes.

Table 3. Extracts potential and IE of the modified SPCE.

| Electrodes | Extracts | E (V) | | | IE ($\mu\text{A/V}$) |
|---|-------------|----------------|----------------|----------------|------------------------|
| | | E ₁ | E ₂ | E ₃ | |
| Pt/C | pomegranate | 0.2 | 0.39 | 0.55 | 52.51 ± 6.00 |
| | hibiscus | 0.22 | 0.40 | - | 54.84 ± 8.37 |
| | pitaya | 0.24 | - | - | 65.92 ± 7.52 |
| $\text{Pt}_{80\%}\text{Ru}_{20\%}/\text{C}$ | pomegranate | 0.15 | 0.39 | 0.65 | 104.79 ± 6.89 |
| | hibiscus | 0.19 | 0.39 | 0.64 | 117.88 ± 9.78 |
| | pitaya | 0.19 | 0.65 | - | 66.87 ± 4.52 |
| $\text{Pt}_{60\%}\text{Ru}_{40\%}/\text{C}$ | pomegranate | 0.15 | 0.39 | 0.64 | 74.48 ± 5.94 |
| | hibiscus | 0.20 | 0.40 | 0.64 | 154.96 ± 5.34 |
| | pitaya | 0.26 | 0.68 | - | 81.03 ± 7.05 |

Using a Shirley-type background for the spectra and a standard Gaussian-Lorentzian (GL) line shape fitting for the high-resolution data, we were able to evaluate the surface composition, oxidation state, and charge transfer tendencies between the electrocatalysts components by XPS [27]. The high-resolution spectrum obtained for Pt (Figure 6A,B) showed binding energies (B.E.) for Pt^0 and Pt^{2+} species for both materials. However, completely different $\text{Pt}^{2+}/\text{Pt}^0$ ratios were observed, according to Table 4. Analyses showed an unexpected outcome. The catalyst without Ru presented a higher content of the reduced Pt species. On the contrary, the sample with Ru 40.0 at.% addition showed more oxidized Pt species. Although it is just a possibility, we can suggest that the oxidized Pt species content could affect the materials' performance, explaining the previously observed data.

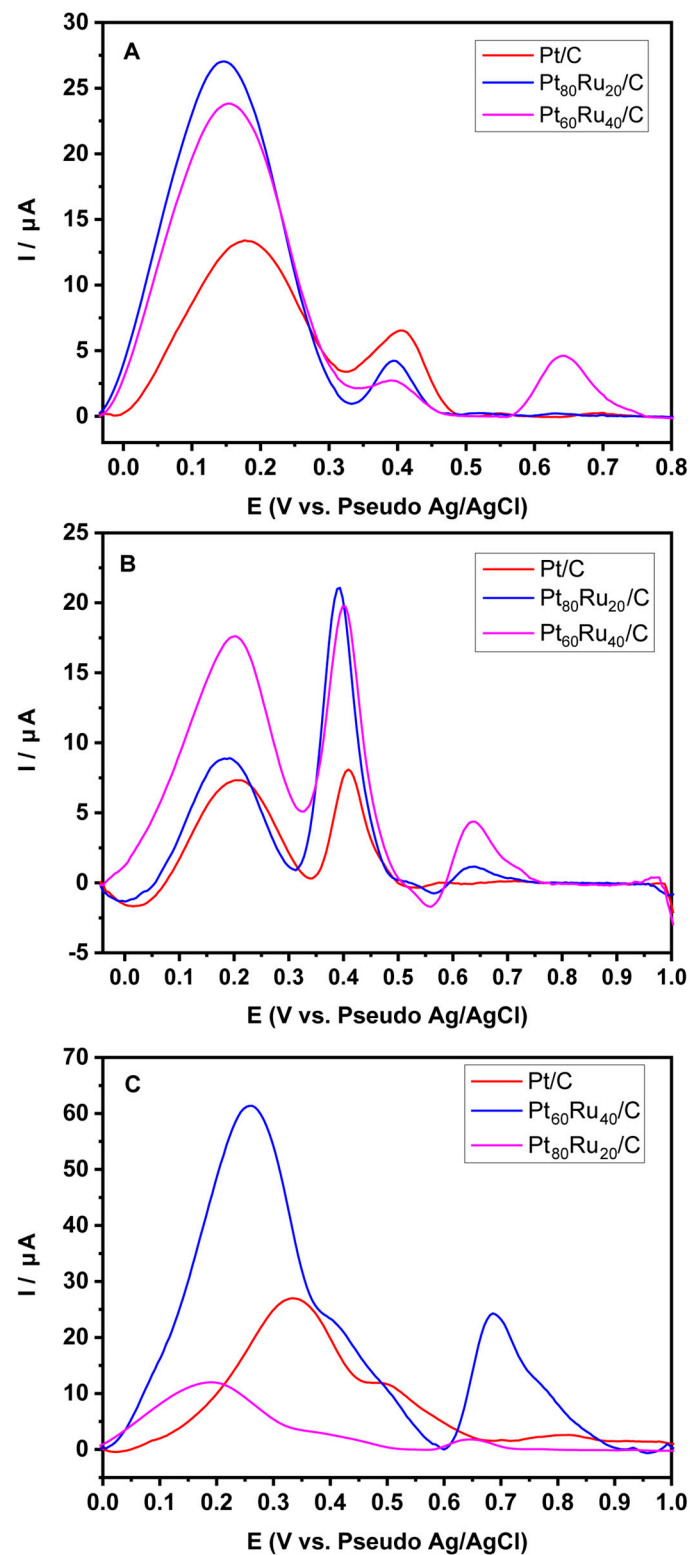


Figure 5. DPV tests performed with the modified electrodes for (A) pitaya, (B) hibiscus, and (C) pomegranate in HCl/KCl 0.2 mol L^{-1} , $v = 10 \text{ mV/s}$.

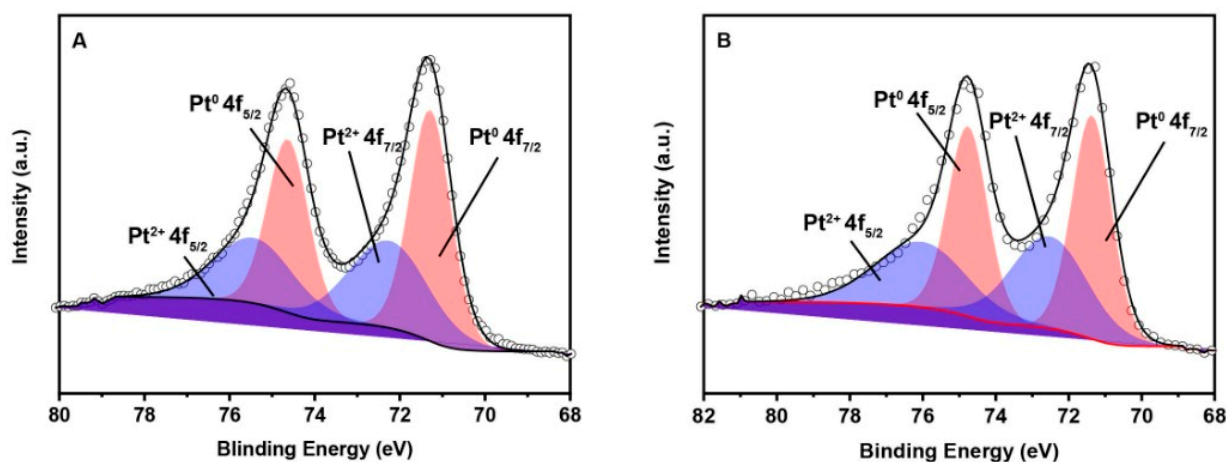


Figure 6. XPS Analyses show the Pt 4f regions of (A) Pt/C and (B) Pt₆₀Ru₄₀/C electrocatalysts.

Table 4. XPS data for the electrocatalysts.

| Samples | Pt 4f _{7/2} | Pt 4f _{5/2} | Pt ²⁺ /Pt ⁰ |
|--------------------------------------|----------------------|----------------------|-----------------------------------|
| Pt/C | 71.3 | 74.6 | 0.74 |
| Pt ₆₀ Ru ₄₀ /C | 71.3 | 74.6 | 1.68 |

4. Conclusions

In the present article, we proposed the modification of SPCE with mono- and bimetallic electrocatalysts based on Pt (or Pt/Ru) supported on Vulcan XC-72 to evaluate the antioxidant capacity of extracts of pomegranate, hibiscus, and pitaya by the electrochemical quantitative index. Initially, we considered rutin and catechin as standards on unmodified and modified SPCE to assess the performance of metal-based materials. Interestingly, the antioxidant evaluation of the materials was remarkably different when the Pt/C was used; however, the bimetallic catalysts were even more sensitive. When the natural extracts were used, the trend was similar, reaching higher EI values with the modified SPCE with the bimetallic materials, which was quite interesting, considering that the metal content was very low as the modification process used a small amount of the prepared materials. We also observed that the material with a higher content of Ru presented the best performance in two of the extracts. XPS analysis showed that the Pt oxidation state was different when Ru was in the material, which could have affected the obtained results. These results showed the excellent electrochemical detection sensitivity and the suitability of the electrochemistry method for detecting low levels of electroactive phenolic compounds without the need to utilize other methods, such as chromatographic techniques. Although we believe that we could progress in the field by showing how the present electrocatalysts can be considered for detecting the total antioxidant capacity of natural extracts, some shortcomings were raised in the studies: (1) the electrode cannot be used several times; (2) we used two noble metals, which are in very low concentrations, however, may be considered not cost-effective by some. Then, future experiments will be performed to decrease their concentration over the carbon; (3) we can see the total concentration of the antioxidants, but we do not detect individual molecules, just a majority of them (several different molecules). Future studies are aiming to improve such results.

Supplementary Materials: The following supporting information can be downloaded at: <https://www.mdpi.com/article/10.3390/chemosensors11060314/s1>, Figure S1: TEM and selected area electron diffraction of (A, B) Pt/C, (D, E) Pt₈₀Ru₂₀/C, and (G, H) Pt₆₀Ru₄₀/C electrocatalysts; Table S1: Particle size obtained by the Scherrer equation.

Author Contributions: G.C.D.: Investigation, Formal Analysis. V.T.R.P.G. and R.B.d.L.: Writing—Review and Editing. M.d.A., S.J.A.F., I.F.T., L.G.d.F.B. and H.A.V.: Investigation, Formal Analysis. M.A.S.G.: Writing—Original draft preparation. I.d.A.R.: Conceptualization, Writing—Review Supervision. All authors have read and agreed to the published version of the manuscript.

Funding: The authors acknowledge the financial support of Fundação de Amparo à Pesquisa e ao Desenvolvimento Científico e Tecnológico do Maranhão (FAPEMA) and Coordenação de Aperfeiçoamento de Pessoal de Nível Superior—Brasil (CAPES)—Finance Code 001 (CAPES Portaria n° 206, de 4 de setembro de 2018). M.A. was supported by the Margarita Salas postdoctoral contract MGS/2021/21 (UP2021-021) financed by the European Union-Next Generation EU.

Institutional Review Board Statement: Not applicable.

Informed Consent Statement: Not applicable.

Data Availability Statement: Not applicable.

Acknowledgments: This research used facilities of the Brazilian Nanotechnology National Laboratory (LNNano), part of the Brazilian Center for Research in Energy and Materials (CNPEM), a private non-profit organization under the supervision of the Brazilian Ministry for Science, Technology, and Innovations (MCTI). Angela Albuquerque from the Spectroscopy and Light Scattering Lab is acknowledged for her assistance during the experiments from proposal 20220969.

Conflicts of Interest: The authors declare that they have no known competing financial interest or personal relationship that could have appeared to influence the work reported in this paper.

References

1. Kotha, R.R.; Tareq, F.S.; Yildiz, E.; Luthria, D.L. Oxidative Stress and Antioxidants—A Critical Review on in vitro Antioxidant Assays. *Antioxidants* **2022**, *11*, 2388. [[CrossRef](#)]
2. Chiorcea-Paquim, A.M.; Enache, T.A.; De Souza Gil, E.; Oliveira-Brett, A.M. Natural phenolic antioxidants electrochemistry: Towards a new food science methodology. *Compr. Rev. Food Sci. Food Saf.* **2020**, *19*, 1680–1726. [[CrossRef](#)] [[PubMed](#)]
3. Munteanu, I.G.; Apetrei, C. Analytical methods used in determining antioxidant activity: A review. *Int. J. Mol. Sci.* **2021**, *22*, 3380. [[CrossRef](#)]
4. Kopustinskiene, D.M.; Jakstas, V.; Savickas, A.; Bernatoniene, J. Flavonoids as Anticancer Agents. *Nutrients* **2020**, *2*, 457. [[CrossRef](#)] [[PubMed](#)]
5. Flieger, J.; Flieger, W.; Baj, J. Antioxidants: Classification, Natural Sources, Activity/Capacity. *Materials* **2021**, *14*, 4135. [[CrossRef](#)] [[PubMed](#)]
6. Zeb, A. Concept, mechanism, and applications of phenolic antioxidants in foods. *J. Food Biochem.* **2020**, *44*, e13394. [[CrossRef](#)] [[PubMed](#)]
7. de Souza, A.C.; Fernandes, A.C.F.; Silva, M.S.; Schwan, R.F.; Dias, D.R. Antioxidant activities of tropical fruit wines. *J. Inst. Brew.* **2018**, *124*, 492–497. [[CrossRef](#)]
8. Granato, D.; Shahidi, F.; Wrolstad, R.; Kilmartin, P.; Melton, L.D.; Hidalgo, F.J.; Miyashita, K.; van Camp, J.; Alasalvar, C.; Ismail, A.B.; et al. Antioxidant activity, total phenolics and flavonoids contents: Should we ban in vitro screening methods? *Food Chem.* **2018**, *264*, 471–475. [[CrossRef](#)]
9. de Araújo Rodrigues, I.; Gomes, S.M.C.; Fernandes, I.P.G.; Oliveira-Brett, A.M. Phenolic Composition and Total Antioxidant Capacity by Electrochemical, Spectrophotometric and HPLC-EC Evaluation in Portuguese Red and White Wines. *Electroanalysis* **2019**, *31*, 936–945. [[CrossRef](#)]
10. Pan, M.; Yang, J.; Liu, K.; Yin, Z.; Ma, T.; Liu, S.; Xu, L.; Wang, S. Noble metal nanostructured materials for chemical and biosensing systems. *Nanomaterials* **2020**, *10*, 209. [[CrossRef](#)]
11. Jiang, K.; Zhang, J.; Chen, J. Enhanced catalytic activity of ternary Pd-Ni-Ir nanoparticles supported on carbon toward formic acid electro-oxidation. *J. Solid State Electrochem.* **2018**, *22*, 1941–1948. [[CrossRef](#)]
12. Goh, A.; Roberts, D.; Wainright, J.; Bhadra, N.; Kilgore, K.; Bhadra, N.; Vrabec, T. Evaluation of Activated Carbon and Platinum Black as High-Capacitance Materials for Platinum Electrodes. *Sensors* **2022**, *22*, 4278. [[CrossRef](#)] [[PubMed](#)]
13. Camara, G.A.; De Lima, R.B.; Iwasita, T. The influence of PtRu atomic composition on the yields of ethanol oxidation: A study by in situ FTIR spectroscopy. *J. Electroanal. Chem.* **2005**, *585*, 128–131. [[CrossRef](#)]
14. Li, C.; Baek, J.B. Recent Advances in Noble Metal (Pt, Ru, and Ir)-Based Electrocatalysts for Efficient Hydrogen Evolution Reaction. *ACS Omega* **2020**, *5*, 31–40. [[CrossRef](#)]
15. Zhao, X.; Zhao, H.; Yan, L.; Li, N.; Shi, J.; Jiang, C. Recent Developments in Detection Using Noble Metal Nanoparticles. *Crit. Rev. Anal. Chem.* **2020**, *50*, 97–110. [[CrossRef](#)]
16. Xia, Y.F.; Guo, P.; Li, J.Z.; Zhao, L.; Sui, X.L.; Wang, Y.; Wang, Z.B. How to appropriately assess the oxygen reduction reaction activity of platinum group metal catalysts with rotating disk electrode. *iScience* **2021**, *24*, 103024. [[CrossRef](#)]

17. França, M.C.; Ferreira, R.M.; Pereira, F.D.S.; e Silva, F.A.; Silva, A.C.A.; Cunha, L.C.S.; Júnior, J.D.J.G.V.; Neto, P.D.L.; Takana, A.A.; Rodrigues, T.S.; et al. Galvanic replacement managing direct methanol fuel cells: AgPt nanotubes as a strategy for methanol crossover effect tolerance. *J. Mater. Sci.* **2022**, *57*, 8225–8240. [[CrossRef](#)]
18. Cardoso, Z.S.; Rodrigues, I.A.; Mendonça, C.J.S.; Rodrigues, J.R.P.; Ribeiro, W.R.A.; Silva, W.O.; Maciel, A.P. Evaluating the electrochemical characteristics of babassu coconut mesocarp ethanol produced to be used in fuel cells. *J. Braz. Chem. Soc.* **2018**, *29*, 1732–1741. [[CrossRef](#)]
19. Issaad, F.Z.; Fernandes, I.P.G.; Enache, T.A.; Mouats, C.; Rodrigues, I.A.; Oliveira-Brett, A.M. Flavonoids in Selected Mediterranean Fruits: Extraction, Electrochemical Detection and Total Antioxidant Capacity Evaluation. *Electroanalysis* **2017**, *29*, 358–366. [[CrossRef](#)]
20. Lima, C.C.; Fonseca, W.S.; Colmati, F.; Ribeiro, L.K.; França, M.C.; Longo, E.; Garcia, M.A.S.; Tanaka, A.A. Enhancing the methanol tolerance of ultrasmall platinum nanoparticles and manganese oxide onto carbon for direct methanol fuel cell: The importance of the synthesis procedure. *Electrochim. Acta* **2020**, *363*, 137256. [[CrossRef](#)]
21. Macêdo, I.; Garcia, L.F.; Neto, J.O.; Leite, K.C.D.S.; Ferreira, V.S.; Ghedini, P.; Gil, E.D.S. Analytical Methods Electroanalytical tools for antioxidant evaluation of red fruits dry extracts. *Food Chem.* **2017**, *217*, 326–331. [[CrossRef](#)] [[PubMed](#)]
22. Song, X.; Wang, D.; Kim, M. Development of an immuno-electrochemical glass carbon electrode sensor based on graphene oxide/gold nanocomposite and antibody for the detection of patulin. *Food Chem.* **2021**, *342*, 128257. [[CrossRef](#)] [[PubMed](#)]
23. de Lima, S.L.S.; Pereira, F.S.; de Lima, R.B.; de Freitas, I.C.; Spadotto, J.; Connolly, B.J.; Barreto, J.; Stavale, F.; Vitorino, H.A.; Fajardo, H.V.; et al. MnO₂-Ir Nanowires: Combining Ultrasmall Nanoparticle Sizes, O-Vacancies, and Low Noble-Metal Loading with Improved Activities towards the Oxygen Reduction Reaction. *Nanomaterials* **2022**, *12*, 3039. [[CrossRef](#)] [[PubMed](#)]
24. Wang, H.; Sun, S.; Mohamedi, M. Synthesis of free-standing ternary Rh-Pt-SnO₂-carbon nanotube nanostructures as a highly active and robust catalyst for ethanol oxidation. *RSC Adv.* **2020**, *10*, 45149–45158. [[CrossRef](#)] [[PubMed](#)]
25. Tajik, S.; Beitollahi, H.; Shahsavari, S.; Nejad, F.G. Simultaneous and selective electrochemical sensing of methotrexate and folic acid in biological fluids and pharmaceutical samples using Fe₃O₄/ppy/Pd nanocomposite modified screen printed graphite electrode. *Chemosphere* **2022**, *291*, 132736. [[CrossRef](#)]
26. Ruiz-Caro, P.; Espada-Bellido, E.; García-Guzmán, J.J.; Bellido-Milla, D.; Vázquez-González, M.; Cubillana-Aguilera, L.; Palacios-Santander, J.M. An electrochemical alternative for evaluating the antioxidant capacity in walnut kernel extracts. *Food Chem.* **2022**, *393*, 133417. [[CrossRef](#)]
27. Major, G.H.; Fairley, N.; Sherwood, P.M.A. Practical guide for curve fitting in x-ray photoelectron spectroscopy. *J. Vac. Sci. Technol. A* **2020**, *38*, 61203. [[CrossRef](#)]

Disclaimer/Publisher's Note: The statements, opinions and data contained in all publications are solely those of the individual author(s) and contributor(s) and not of MDPI and/or the editor(s). MDPI and/or the editor(s) disclaim responsibility for any injury to people or property resulting from any ideas, methods, instructions or products referred to in the content.